Genetic mapping of sex and self-incompatibility determinants in the androdioecious plant *Phillyrea angustifolia*

Authors:
Amélie Carré[1], Sophie Gallina[1], Sylvain Santoni[2], Philippe Vernet[1], Cécile Godé[1], Vincent Castric[1], Pierre Saumitou-Laprade[1#]

Affiliations :
[1] CNRS, Univ. Lille, UMR 8198 – Evo-Eco-Paleo, F-59000 Lille, France
[2] UMR DIAPC - Diversité et adaptation des plantes cultivées

[#] **Corresponding author**: Pierre.Saumitou-Laprade@univ-lille.fr

Abstract

The diversity of mating and sexual systems in Angiosperms is spectacular, but the factors driving their evolution remain poorly understood. In plants of the Oleaceae family, an unusual self-incompatibility (SI) system has been discovered recently, whereby only two distinct homomorphic SI specificities segregate stably. To understand the role of this peculiar SI system in preventing or promoting the diversity of sexual phenotypes observed across the family, an essential first step is to characterize the genetic architecture of these two traits. Here, we developed a high-density genetic map of the androdioecious shrub *P. angustifolia* based on a F1 cross between a hermaphrodite and a male parent with distinct SI genotypes. Using a double restriction-site associated digestion (ddRAD) sequencing approach, we obtained reliable genotypes for 196 offspring and their two parents at 10,388 markers. The resulting map comprises 23 linkage groups totaling 1,855.13 cM on the sex-averaged map. We found strong signals of association for the sex and SI phenotypes, that were each associated with a unique set of markers on linkage group 12 and 18 respectively, demonstrating inheritance of these traits as single, independent, mendelian factors. The *P. angustifolia* linkage map shows robust synteny to the olive tree genome overall. Two of the six markers strictly associated with SI in *P. angustifolia* have strong similarity with a recently identified 741kb chromosomal region fully linked to the SI phenotype on chromosome 18 of the olive tree genome, providing strong cross-validation support. The SI locus stands out as being markedly rearranged, while the sex locus has remained relatively more collinear between the two species. This *P. angustifolia* linkage map will be a useful resource to investigate the various ways by which the sex and SI determination systems have co-evolved in the broader phylogenetic context of the Oleaceae family.

Introduction

Sexual reproduction is strikingly diverse across Angiosperms, both in terms of the proportion of autogamous vs. allogamous matings and in terms of the distribution of male and female sexual functions within and among individuals (BARRETT 1998; SAKAI AND WELLER 1999; DIGGLE *et al.* 2011). The conditions under which this diversity could arise under apparently similar ecological conditions and have evolved rapidly -sometimes even within the same family- have been a topic of intense interest in evolutionary biology (BARRETT 1998). The control of self-fertilization and the delicate balance between its costs and benefits is considered to be a central force driving this diversity. Avoidance of self-fertilization is sometimes associated with observable phenotypic variations among reciprocally compatible partners. These variations can be morphological (e.g. distyly) or temporal (e.g. protandry, protogyny in the case of heterodichogamy), but in many cases the flowers show no obvious morphological or phenological variation, and self-fertilization avoidance relies on so-called "homomorphic" self-incompatibility (SI) systems. These systems are defined as the inability of fertile hermaphrodite plants to produce zygotes through self-fertilization (LUNDQVIST 1956; DE NETTANCOURT 1977), and typically rely on the segregation of a finite number of recognition "specificities" whereby matings between individuals expressing cognate specificities are not successful at producing zygotes. At the genetic level, the SI specificities most commonly segregate as a single multi-allelic mendelian locus, the S locus. This locus contains at least two genes, one encoding the male determinant expressed in pollen and the other encoding the female determinant expressed in pistils, with the male specificity sometimes determined by a series of tandemly arranged paralogs (KUBO *et al.* 2015). The male and female determinants are both highly polymorphic and tightly linked, being inherited as a single non-recombining genetic unit. In cases where the molecular mechanisms controlling SI could be studied in detail, they were found to be remarkably diverse, illustrating their independent evolutionary origins across the flowering plants (IWANO AND TAKAYAMA 2012). Beyond the diversity of the molecular functions employed, SI systems can also differ in their genetic architecture.

In the Poaceae family for example, two independent loci (named S and Z) control SI (Yang, et al., 2008). In other cases, the alternate allelic specificities can be determined by presence-absence variants rather than nucleotide sequence variants of a given gene, such as *e.g.* in *Primula vulgaris*, where one of the two reproductive phenotypes is hemizygous rather than heterozygous for the SI locus (LI *et al.* 2016).

In spite of this diversity of molecular mechanisms and genetic architectures, a common feature of SI phenotypes is that they are all expected to evolve under negative frequency-dependent selection, a form of natural selection favoring the long-term maintenance of high levels of allelic diversity (WRIGHT 1939). Accordingly, large numbers of distinct SI alleles are commonly observed to segregate within natural and cultivated SI species (reviewed in CASTRIC AND VEKEMANS 2004). There are notable exceptions to this general rule, however, and in some species only two SI specificities seem to segregate stably. Most often in such diallelic SI systems, the two SI specificities are in perfect association with morphologically distinguishable floral phenotypes. In distylous species, for instance, two floral morphs called “pin” (L-morph) and “thrum” (S-morph) coexist (BARRETT 1992; BARRETT 2019). In each morph, the anthers and stigma are spatially separated within the flowers, but located at corresponding, reciprocal positions between the two morphs. Additional morphological differences exist, with S-morph flowers producing fewer but larger pollen grains than L-morph flowers (DULBERGER 1992). These morphological differences are believed to enhance the selfing avoidance conferred by the SI system but also to increase both male and female fitnesses (BARRETT 1990; BARRETT 2002; KELLER *et al.* 2014), although it is not clear which of SI or floral morphs became established in the first place (CHARLESWORTH AND CHARLESWORTH 1979).

The Oleacea family is another intriguing exception, where a diallelic SI system was recently found to be shared across the entire family (VERNET *et al.* 2016). In this family of trees, the genera *Jasminum* (2*n* = 26), *Fontanesia* (2*n* = 26) and *Forsythia* (2*n*= 28) are all heterostylous and are therefore all expected to possess a heteromorphic diallelic SI system; in *Jasminum fruticans* self- and within-morph fertilization are unsuccessful (DOMMÉE *et al.* 1992). The ancestral heterostyly gave rise to species with hermaphrodite (e.g.

Ligustrum vulgare, *Olea europaea*), androdioecious (e.g. *P. angustifolia*, *Fraxinus ornus*), polygamous (e.g. *Fraxinus excelsior*) and even dioecious (e.g. *Fraxinus chinensis*) sexual systems, possibly in association with a doubling of the number of chromosomes (2*n*= 46 in the Oleeae tribe). Evaluation of pollen germination success by controlled *in vitro* crossing experiments (stigma test) revealed the existence of a previously unsuspected homomorphic diallelic SI, in one of these species, P. angustifolia (SAUMITOU-LAPRADE *et al.* 2010). In this androdioecious species (i.e. in which male and hermaphrodite individuals coexist in the same populations), hermaphrodite individuals form two morphologically indistinguishable groups of SI specificities that are reciprocally compatible but incompatible within groups, whereas males show compatibility with hermaphrodites of both groups (SAUMITOU-LAPRADE *et al.* 2010). This "universal" compatibility of males offsets the reproductive disadvantage they suffer from lack of their female function, such that the existence of the diallelic SI system provides a powerful explanation to the long-standing evolutionary puzzle represented by the maintenance of high frequencies of males in this species (PANNELL AND KORBECKA 2010; SAUMITOU-LAPRADE *et al.* 2010; BILLIARD *et al.* 2015; PANNELL AND VOILLEMOT 2015). Extension of the stigma test developed in *P. angustifolia* to other species of the same tribe including *L. vulgaris* (DE CAUWER *et al.* 2020), *F. ornus* (VERNET *et al.* 2016) and *O. europaea* (SAUMITOU-LAPRADE *et al.* 2017; DUPIN *et al.* 2020) demonstrated that all species exhibited some form of the diallelic SI system, but with no consistent association with floral morphology. Cross-species pollination experiments even showed that pollen from *P. angustifolia* is able to trigger a robust SI response on *O. europaea* and the more distant *F. ornus* and *F. excelsior* stigmas (the reciprocal is also true). This opens the question of whether the homomorphic diallelic SI determinants are orthologs across the Oleeae tribe, even in the face of the variety of sexual polymorphisms present in the different species. More broadly, its link with the heteromorphic diallelic SI determinant in the ancestral diploid, largely heterostylous, species remains to be established (BARRETT 2019). Understanding the causes of the long-term maintenance of this SI system and exploring its consequences on the evolution of sexual systems in hermaphrodite, androdioecious, polygamous or

109 dioecious species of the family represents an important goal. The case of *P. angustifolia* is particularly
110 interesting because it is one of the rare instances where separate sexes decoupled from mating types can
111 be studied in a single species (CHARLESWORTH 1978).

112 A first step toward a better understanding of the role of the diallelic SI system in promoting the
113 sexual diversity in Oleaceae is to characterize and compare the genetic architecture of the SI and sexual
114 phenotypes. At this stage, however, the genomic resources for most of these non-model species remain
115 limited. In this context, the recent sequencing efforts (UNVER *et al.* 2017; JIMÉNEZ-RUIZ *et al.* 2020) and the
116 genetic mapping of the SI locus in a biparental population segregating for SI groups in *Olea europaea*
117 (MARIOTTI *et al.* 2020) represent major breakthroughs in the search for the SI locus in Oleaceae. They have
118 narrowed down the SI locus to an interval of 5.4cM corresponding to a region of approximately 300kb, but
119 it is currently unknown whether the same region is controlling SI in other species. In *P. angustifolia,* based
120 on a series of genetic analysis of progenies from controlled crosses, Billiard *et al.* (2015) proposed a fairly
121 simple genetic model, where sex and SI are controlled by two independently segregating diallelic loci.
122 Under this model, sex would be determined by the "M" locus at which a dominant allele *M* codes for the
123 male phenotype (*i.e. M is a* female-sterility mutation leading e.g. to arrested development of the stigma)
124 and a recessive allele *m* codes for the hermaphrodite phenotype. The S locus would encode the SI system
125 and comprise a dominant allele *S2* and a recessive allele *S1.* The model thus hypothesizes that
126 hermaphrodites are homozygous *mm* at the sex locus, and fall into two groups of SI specificities, named
127 H_a and H_b carrying the *S1S1* and *S1S2* genotypes at the S locus, respectively (their complete genotypes
128 would thus be *mmS1S1* and *mmS1S2* respectively). The model also hypothesizes three male genotypes
129 (M_a: *mMS1S1*, M_b: *mMS1S2*, and M_c*: mMS2S2*). In addition, Billiard *et al.* (2015) showed that, while males
130 are compatible with all hermaphrodites, the segregation of sexual phenotypes varies according to which
131 group of hermaphrodites they sire: the progeny of H_a hermaphrodites pollinated by males systematically
132 consists of both hermaphrodites and males with a consistent but slight departure from 1:1 ratio, while

133 that of H_b hermaphrodites pollinated by the very same males systematically consists of male individuals
134 only. This observation suggests a pleiotropic effect of the *M* allele, conferring not only female sterility and
135 universal pollen compatibility, but also a complete male-biased sex-ratio distortion when crossed with one
136 of the two groups of hermaphrodites and a more subtle departure from 1:1 ratio when crossed with the
137 other group of hermaphrodites (BILLIARD *et al.* 2015). The latter departure, however, was observed on
138 small progeny arrays only, and its magnitude thus comes with considerable uncertainty.

139 In this study, we developed a high-density genetic map for the non-model tree *P. angustifolia* using
140 a ddRAD sequencing approach and used it to address three main questions related to the evolution of its
141 peculiar reproductive system. First, are the SI and sex phenotypes in *P. angustifolia* encoded by just two
142 independent loci, as predicted by the most likely segregation model of Billiard *et al.* (2015)? Second, which
143 specific genomic regions are associated with the SI and sex loci, and what segregation model do the SI and
144 sex-associated loci follow (i.e. which of the males or hermaphrodites, and which of the two SI phenotypes
145 are homozygous *vs.* heterozygous at either loci, or are these phenotypes under the control of hemizygous
146 genomic regions?). Third, what is the level of synteny between our *P. angustifolia* genetic map and the
147 recently published Olive tree genome (UNVER *et al.* 2017; MARIOTTI *et al.* 2020), both globally and
148 specifically at the SI and sex-associated loci?

149

150 ## Material and Methods

151 ### Experimental cross and cartography population

152 In order to get both the SI group and the sexual phenotype (males vs hermaphrodites) to segregate
153 in a single progeny array, a single maternal and a single paternal plant were chosen among the progenies
154 of the controlled crosses produced by (BILLIARD *et al.* 2015). Briefly, a H_a maternal tree (named 01.N-25,
155 with putative genotype mmS1S1) was chosen in the progeny of a (H_a x M_a) cross. It was crossed in March
156 2012 to a M_b father (named 13.A-06, putative genotype mM S1S2) chosen in the progeny of a (H_a x M_c)
157 cross, following the protocol of Saumitou-Laprade *et al.* (2010). Both trees were maintained at the

158 experimental garden of the "Plateforme des Terrains d'Expérience du LabEx CeMEB," (CEFE, CNRS) in
159 Montpellier, France. F1 seeds were collected in September 2012 and germinated in the greenhouse of the
160 "Plateforme Serre, cultures et terrains expérimentaux," at the University of Lille (France). Seedling
161 paternity was verified with two highly polymorphic microsatellite markers (VASSILIADIS *et al.* 2002), and
162 1,064 plants with confirmed paternity were installed in May 2013 on the experimental garden of the
163 "Plateforme des Terrains d'Expérience du LabEx CeMEB," (CEFE, CNRS) in Montpellier. Sexual phenotypes
164 were visually determined based on the absence of stigma for 1,021 F1 individuals during their first
165 flowering season in 2016 and 2017 (absence of stigma indicates male individuals). Twenty-one progenies
166 did not flower and 22 died during the test period. The hermaphrodite individuals were assigned to an SI
167 group using the stigma test previously described in Saumitou-Laprade *et al.* (2010; SAUMITOU-LAPRADE *et al.*
168 2017).
169

170 **DNA extraction, library preparation and sequencing**

171 In 2015, *i.e.* the year before sexual phenotypes were determined and stigma tests were
172 performed, 204 offspring were randomly selected for genomic library preparation and genotyping. Briefly,
173 DNA from parents and progenies was extracted from 100 mg of frozen young leaves with the Chemagic
174 DNA Plant Kit (Perkin Elmer Chemagen, Baesweller, DE, Part # CMG-194), according to the manufacturer's
175 instructions. The protocol was adapted to the use of the KingFisher Flex™ (Thermo Fisher Scientific,
176 Waltham, MA, USA) automated DNA purification workstation. The extracted DNA was quantified using a
177 Qubit fluorometer (Thermo Fisher Scientific, Illkirch, France). Genome complexity was reduced by Double
178 Digestion Restriction Associated DNA sequencing (ddRAD seq) (PETERSON *et al.* 2012) using two restriction
179 enzymes: *PstI*, a rare-cutting restriction enzyme sensitive to methylation recognizing the motif CTGCA/G,
180 and *MseI*, a common-cutting restriction enzyme (recognizing the motif T/TAA). The libraries were
181 constructed at the INRAE - AGAP facilities (Montpellier, France). Next-generation sequencing was

182 performed in a 150-bp paired-ends-read mode using three lanes on a HiSeq3000 sequencer (Illumina, San
183 Diego, CA, USA) at the Get-Plage core facility (Genotoul platform, INRAE Toulouse, France).
184

185 **GBS data analysis and linkage mapping**

186 Illumina sequences were quality filtered with the *process_radtags* program of Stacks v2.3
187 (CATCHEN *et al.* 2011) to remove low quality base calls and adapter sequences. We followed the Rochette
188 & Catchen protocol (ROCHETTE AND CATCHEN 2017) to obtain a *de novo* catalog of reference loci. Briefly, the
189 reads were assembled and aligned with a minimum stack depth of 3 (–m=3) and at most two nucleotide
190 differences when merging stacks into loci (–M=2). We allowed at most two nucleotide differences between
191 loci when building the catalog (–n=2). Both parental and all offspring FASTQ files were aligned to the *de*
192 *novo* catalog using Bowtie2 v2.2.6 (LANGMEAD AND SALZBERG 2012), the option 'end-to-end' and 'sensitive'
193 were used for the alignment. At this step, one .bam file was obtained per individual to construct the linkage
194 map with Lep-MAP3 (RASTAS 2017). A custom python script was used to remove SPNs markers with reads
195 coverage <5. After this step, the script calls Samtools v1.3.1 and the script *pileupParser2.awk* (limit1=5) to
196 convert *.bam* files to the format used by Lep-MAP3. We used the *ParentCall2* module of Lep-MAP3 to
197 select loci with reliable parental genotypes by considering genotype information on parents and offspring.
198 The *Filtering2* module was then used to remove non-informative and distorted markers (dataTolerance =
199 0.0000001). The module *SeparateChromosomes2* assigned markers to linkage groups (LGs), after test,
200 where the logarithm of odds score (LodLimit) varied from 10 to 50 in steps of 5 then from 20 to 30 in steps
201 of 1 and the minimum number of SNP markers (sizeLimit) per linkage group from 50 to 500 in steps of 50
202 for each of the LodLimit. The two parameters, lodLimit = 27 and sizeLimit = 250, were chosen as the best
203 parameters to obtain the 23 linkage groups (as expected in members of the Oleoideae subfamily;
204 WALLANDER AND ALBERT 2000). A custom python script removed loci with SNPs markers mapped on two or
205 more different linkage groups. The last module *OrderMarkers2* ordered the markers within each LG. To

206 consider the slight stochastic variation in marker distances between executions, the module was run three
207 times on each linkage group, first separately for the meiosis that took place in each parent (sexAveraged
208 = 0) and then averaged between the two parents (sexAveraged = 1). To produce the most likely final father
209 and mother specific maps and a final sex-averaged maps (De-Kayne and Feulner 2018), we kept for each
210 map the order of markers that had the highest likelihoods for each linkage group. In the end of some
211 linkage groups, we removed from the final genetic map markers that were clearly outliers i.e. that had
212 orders of magnitude more recombination to any marker than the typical average (Table 1). The original
213 map is provided in Figure S1.

214

215 **Sex and SI locus identification**

216 To identify the sex-determination system in *P. angustifolia* we considered two possible genetic
217 models. First, a "XY" male heterogametic system, where males are heterozygous or hemizygous (XY) and
218 hermaphodites are homozygous (XX). Second, a "ZW" hermaphrodite heterogametic system, where
219 hermaphodites are heterozygous or hemizygous (ZW) and males are homozygous (ZZ). We applied the
220 same logic to the SI determination system, as segregation patterns (Billiard et al. 2015) suggested that SI
221 possibly also has a heterogametic determination system, with homozygous H_a and heterozygous H_b. In the
222 same way as for sex, it is therefore possible to test the different models (XY, ZW or hemizygous) to
223 determine which SNPs are linked to the two SI phenotypes.

224 Based on this approach, we identified sex-linked and SI-linked markers on the genetic map by
225 employing SEX-DETector, a maximum-likelihood inference model initially designed to distinguish
226 autosomal from sex-linked genes based on segregation patterns in a cross (Muyle *et al.* 2016). Briefly, a
227 new alignment of reads from each individual on the loci used to construct the linkage map was done with
228 bwa (Li and Durbin 2009). This new alignment has the advantage of retrieving more SNPs than used by
229 LepMap3, as SNPs considered as non-informative by LepMap3 can still be informative to distinguish among

230 sex- or SI-determination systems by SEX-DETector. The alignment was analyzed using Reads2snp (default
231 tool for SEX-DETector) (TSAGKOGEORGA *et al.* 2012) with option -par 0. We ran Reads2snp without the -aeb
232 (account for allelic expression bias) option to accomodate for the use of genomic rather than RNA-seq
233 data. For each phenotype (H_a vs. H_b and males vs. hermaphrodites), SEX-DETector was run for both a XY
234 and a ZW model with the following parameters: -detail, -L, -SEM, -thr 0.8, -E 0.05. For each run, SEX-
235 DETector also calculates the probability for X (or Z)-hemizygous segregation in the heterozygous
236 haplotypes. To compensate for the heterogeneity between the number of males (83) and hermaphrodites
237 (113) in our progeny array, each model was tested three times with sub-samples of 83 hermaphrodites
238 obtained by randomly drawing from the 113 individuals. We retained SNPs with a ≥80% probability of
239 following an XY (or ZW) segregation pattern, with a minimum of 50% of genotyped individuals and less
240 that 5% of the individuals departing from this model (due to either genotyping error or crossing-over).
241

242 **Synteny analysis with the olive tree**

243 To study synteny, we used Basic Local Alignment Search Tool (BLAST) to find regions of local
244 similarity between the *P. angustifolia* ddRADseq loci in the linkage map and the *Olea europea var. sylvestris*
245 genome assembly (UNVER *et al.* 2017). This assembly is composed of 23 main chromosomes and a series
246 of 41,233 unanchored scaffolds for a total of 1,142,316,613 bp. Only loci with a unique hit with at least
247 85% identity over a minimum of 110 bp were selected for synteny analysis. Synteny relationships were
248 visualized with *circos-0.69-6* (KRZYWINSKI *et al.* 2009). Synteny between linkage groups of *P. angustifolia*
249 and the main 23 *O. europea* chromosomes was established based on the number of markers with a
250 significant BLAST hit. At a finer scale, we also examined synteny with the smaller unanchored scaffolds of
251 the assembly, as the history of rearrangement and allo-tetraploidization is likely to have disrupted synteny.

252 **Data availability**

253 Fastq files for all 204 offspring and both parents are deposited in the NCBI BioProject (SRA
254 accession PRJNA724813). All scripts used can be accessed at https://github.com/Amelie-Carre/Genetic-
255 map-of-Phillyrea-angustifolia .

256 ## Results

257 ### Phenotyping progenies for sex and SI groups

258 As expected, our cartography population segregated for sex and SI phenotypes, providing a
259 powerful resource to genetically map these two traits. Among the 1,021 F1 individuals that flowered
260 during the two seasons of phenotyping, we scored 619 hermaphrodites and 402 males, revealing a biased
261 sex ratio in favor of hermaphrodites (khi²= 1.28×10^{-11}). Stigma tests were successfully performed on 613
262 hermaphrodites (6 individuals flowered too late to be included in a stigma test), revealing 316 H_a and 297
263 H_b, i.e. an equilibrated segregation of the two SI phenotypes (khi²= 0.27). The random subsample of 204
264 F1 progenies chosen before the first flowering season for ddRAD-seq analysis (see below) followed similar
265 phenotypic proportions. 196 of the 204 progenies ended up flowering, revealing 83 males and 113
266 hermaphrodites, among which 60 belonged to the H_a group and 53 to the H_b group.

267

268 ### Linkage mapping

269 The two parents and the 196 offspring that had flowered were successfully genotyped using a
270 ddRAD-seq approach. Our stringent filtering procedure identified 11,070 loci composed of 17,096 SNP
271 markers as being informative for Lep-MAP3. By choosing a LOD score of 27, 10,388 loci composed of
272 15,814 SNPs were assigned to, and arranged within, 23 linkage groups in both sex-averaged and sex-
273 specific maps (Table 1).

274 The linkage groups of the mother map were on average larger (78.88 cM) than the linkage groups
275 of the father map (73.40 cM) and varied from 22.73 cM to 112.38 cM and from 35 cM to 121.94 cM
276 respectively (Table 1, Figure S1). The total map lengths were 1586.57 cM, 1688.16 cM and 1814.19 cM in
277 the sex-averaged, male and female maps, respectively. The length of the linkage groups varied from 23.90
278 cM to 110.69 cM in the sex-averaged map, with an average of 683 SNPs markers per linkage group (Table
279 1).

280 **Sex and SI locus identification**

281 We found evidence that a region on linkage group 18 (LG18) is associated with the SI phenotypes,
282 with Hb hermaphrodites having heterozygous genotype, akin to a XY system. Indeed, when comparing H_a
283 and H_b, among the 38,998 SNPs analyzed by SEX-DETector, 496 have a probability of following an XY
284 pattern ≥0.80. We then applied two stringent filters by retaining only SNPs that had been genotyped for
285 more than 50% of the offspring (n=211), and for which less than 5% of the offspring departed from the
286 expected genotype under a XY model (n=23). Six of these 23 SNPs, distributed in 4 loci, followed a
287 segregation pattern strictly consistent with a XY model. These four loci are tightly clustered on the linkage
288 map and define a region of 1.230 cM on LG18 (Figure 1) in the sex-averaged map. Relaxing the stringency
289 or our thresholds, this region also contains five loci that strictly follow an XY segregation but with less than
290 50% of offsprings successfully genotyped, as well as six loci with autosomal inheritance, possibly
291 corresponding to polymorphisms accumulated within allelic lineages associated with either of the
292 alternate SI specificities. Using the same filtering scheme, none of the SNPs was found to follow a ZW
293 pattern.

294 For the comparison of male and hermaphrodites, an average of 44,565 SNPs were analyzed by
295 SEX-DETector across the three subsamples, among which an average of 438 have a probability of following
296 an XY pattern ≥0.80. We applied the same set of stringent filters and retained an average of 171 SNPs
297 having been genotyped for at least 50% of the offspring, among which 41 have less than 5% of the offspring
298 departing from the expected genotype under a XY model and are shared across the three subsets. Thirty-
299 two of these SNPs followed a segregation pattern strictly consistent with a XY model. These 32 markers,
300 corresponding to 8 loci, are distributed along a region of 2.216 cM on linkage group 12 (LG12, Figure 1) in
301 the sex-averaged map. Relaxing the stringency or our thresholds, this region also contains five loci that
302 strictly follow an XY segregation pattern but with less than 50% of offspring successfully genotyped, as
303 well as 17 loci consistent with autosomal inheritance, possibly corresponding to polymorphisms

accumulated within allelic lineages associated with either of the alternate sex specificities. Again, no SNP was found to follow a ZW pattern. This provides evidence that this independent region on LG12 is associated with sex, with a determination system akin to a XY system where males have the heterogametic genotype.

Synteny analysis with the olive tree

About half (49%) of the 10,388 *P. angustifolia* loci used for the genetic map had a significant BLAST hit on the olive tree genome. Overall, the relative position of these hits was highly concordant with the structure of the linkage map. Indeed, the vast majority (79.7%) of loci belonging to a given linkage group have non-ambiguous matches on the same olive tree chromosome. Loci that did not follow this general pattern did not cluster on other chromosomes, suggesting either small rearrangements or mapping/assembly errors at the scale of individual loci. The order of loci within the linkage groups was also well conserved with only limited evidence for rearrangements (Figure 2, Figure 3), suggesting that the two genomes have remained largely collinear.

We then specifically inspected synteny between the linkage groups carrying either the sex or the SI locus and the olive tree genome (Figure 4). Synteny was good for LG12, the linkage group containing the markers associated with the sex phenotype. Among the 645 loci of LG12, 365 have good homology in the olive tree genome. Eighty eight percent had their best hits on the same chromosome of the olive tree (chromosome 12 per our numbering of the linkage groups), and the order of markers was largely conserved along this chromosome. Six loci contained in the region associated with sex on LG12 had hits on a single 1,940,009bp region on chromosome 12. This chromosomal interval contains 82 annotated genes in the olive tree genome (Table S1). In addition, eight loci in the sex region had their best hits on a series of five smaller scaffolds (Sca393, Sca1196, Sca1264, Sca32932, Sca969) that could not be reliably anchored in the main olive tree assembly but may nevertheless also contain candidates for sex

328 determination. Collectively, these scaffolds represent 1.849.345bp of sequence in the olive tree genome
329 and contain 57 annotated genes (Table S1).

330 Synteny was markedly poorer for markers on LG18, the linkage group containing the markers
331 associated with the SI specificity phenotypes (Figure 5). Of the 440 loci on LG18, 203 have non-ambiguous
332 BLAST hits on the olive tree genome. Although a large proportion (89%) had their best hits on chromosome
333 18, the order of hits along that chromosome suggested a large number of rearrangements. This more
334 rearranged order was also observed for the six markers that were strictly associated with SI in *P.*
335 *angustifolia*. Two of them had hits on a single region of 741,403bp on the olive tree genome. This region
336 contains 32 annotated genes (Table S2) and contains two markers that were previously found to be
337 genetically associated with SI directly in the olive tree by Mariotti *et al.* (2020). Three markers more loosely
338 associated with SI in *P. angustifolia* found hits on a more distant region on chromosome 18 (19,284,909-
339 19,758,630Mb). The three other strongly associated markers all had hits on scaffold 269, which contains
340 15 annotated genes and represents 545,128bp. Nine other loci strongly or loosely associated with SI had
341 hits on a series of seven other unanchored scaffolds (Sca1199, Sca1200, Sca1287, Sca1579, Sca213,
342 Sca327, Sca502) that collectively represent 96 annotated genes (Table S2) and 2,539,637bp.

343

344 Discussion

345 Until now, studies have mostly relied on theoretical or limited genetic segregation analyses to
346 investigate the evolution of sexual and SI phenotypes in *P. angustifolia* (VASSILIADIS *et al.* 2002; SAUMITOU-
347 LAPRADE *et al.* 2010; HUSSE *et al.* 2013; BILLIARD *et al.* 2015). In this study, we created the first genetic map
348 of the androdioecious species *P. angustifolia* and identified the genomic regions associated with these two
349 important reproductive phenotypes. The linkage map we obtained shows strong overall synteny with the
350 olive tree genome, and reveals that sex and SI phenotypes segregate independently from one another,
351 and are each strongly associated with a different genomic region (in LG18 and LG12, respectively).

352 The SI linked markers on LG18 are orthologous with the genomic interval recently identified by
353 Mariotti *et al.* (2020) as the region controlling SI in the domesticated olive tree, providing strong reciprocal
354 support that the determinants of SI are indeed located in this region. Interestingly, we observed a series
355 of shorter scaffolds that could not previously be anchored in the main assembly of the olive tree genome
356 but match genetic markers that are strictly linked to SI in *P. angustifolia.* These unanchored scaffolds
357 provide a more complete set of genomic sequences that will be important to consider in the perspective
358 of identifying the (currently elusive) molecular determinants of SI in these two species. We note that poor
359 assembly of the S-locus region (MARIOTTI *et al.* 2020) was expected given the considerable levels of
360 structural rearrangements typically observed in SI- and more generally in the mating type-determining
361 regions (GOUBET *et al.* 2012; BADOUIN *et al.* 2015), making *P. angustifolia* a useful resource to map the SI
362 locus in the economically important species *O. europeae*.

363 Our observations also provide direct support to the hypothesis that the determinants of SI have
364 remained at the same genomic position at least since the two lineages diverged, 30 to 40 Myrs ago
365 (BESNARD *et al.* 2009; OLOFSSON *et al.* 2019). Stability of the genomic location of SI genes has been observed
366 in some Brassicaceae species, where the *SRK-SCR* system maps at orthologous positions in the Arabidopsis
367 and Capsella genuses (GUO *et al.* 2011). In other Brassicaceae species, however, the SI system is found at
368 different genomic locations, such as in Brassica and Leavenworthia. In the former, the molecular
369 determinants have remained orthologous (also a series of *SRK-SCR* pairs, (IWANO *et al.* 2014), but not in
370 the latter, where SI seems to have evolved d*e novo* from exaptation of a pair of paralogous genes (CHANTHA
371 *et al.* 2013; CHANTHA *et al.* 2017). Together with the fact that *P. angustifolia* pollen is able to trigger a robust
372 SI response on *O. europaeae* stigmas (SAUMITOU-LAPRADE *et al.* 2017), our results provide strong support to
373 the hypothesis that the *P. angustifolia* and *O. europaeae* SI systems are orthologous.

374 Several approaches could now be used to refine the mapping location in *P. angustifolia,* and
375 ultimately zero in on the molecular determinants of SI. One possibility would require fine-mapping using

376 larger offspring arrays, starting from our cross for which only a fraction of all phenotyped individuals were
377 genotyped. Beyond the analysis of this controlled cross, evaluating whether the association of the SI
378 phenotype still holds for markers within a larger set of accessions from diverse natural populations will
379 constitute a powerful fine-mapping approach. Since the SI phenotypes seem to be functionally
380 orthologous across the Oleeae tribe (VERNET *et al.* 2016), the approach could, in principle, be extended to
381 more distant SI species of the family like *L. vulgare* or *F. ornus*. Identification of sequences that have
382 remained linked over these considerable time scales would represent excellent corroborative evidence to
383 validate putative SI candidates. In parallel, an RNA-sequencing approach could be used to identify
384 transcripts specific to the alternate SI phenotypes.

385 While comparison to the closely related *O. europeae* genome is a useful approach for the mapping
386 of SI in *P. angustifolia*, it is *a priori* of limited use for mapping the sex-determining region, since the olive
387 tree lineage has been entirely hermaphroditic for at least 32.22 Myrs (confidence interval: 28-36 Myrs)
388 (FigS1 in OLOFSSON *et al.* 2019). Detailed exploration of the genomic region in the olive tree that is
389 orthologous to the markers associated with sex in *P. angustifolia* is however interesting, as it may either
390 have anciently played a role in sex determination and subsequently lost it, or alternatively it may contain
391 quiescent sex-determining genes that have been activated specifically in *P. angustifolia*. At a broader scale,
392 mapping and eventually characterizing the sex locus in other androdioecious species such as e.g. *F. ornus*
393 could indicate whether the different instances of androdioecy in the family represent either orthologous
394 phenotypes or independent evolutionary emergences.

395 Identifying the molecular mechanisms of the genes controlling SI and sex and tracing their
396 evolution in a phylogenetic context would prove extremely useful. First, it could help understand the
397 strong functional pleiotropy between sex and SI phenotypes, whereby males express universal SI
398 compatibility (SAUMITOU-LAPRADE *et al.* 2010). In other words, males are able to transmit the SI specificities
399 they inherited from their parents, but they do not express them themselves even though their pollen is

400 fully functional. This intriguing feature of the SI system was key to solve the puzzle of why *P. angustifolia*
401 maintains unusually high frequencies of males in natural populations (HUSSE *et al.* 2013), but the question
402 of how being a male prevents expression of the SI phenotype in pollen is still open. A possibility is that the
403 *M* allele of the sex locus contains a gene interacting negatively either with the pollen SI determinant itself
404 or with a gene of the downstream response cascade. Identifying the molecular basis of this epistasis will
405 be an interesting next step. Second, another intriguing feature of the system is segregation distortion, that
406 is observed at several levels. Billiard *et al.* (2015) observed complete segregation bias in favor of male
407 offspring of H_b hermaphrodites sired by males. Here, by phenotyping >1,000 offspring of a H_a
408 hermaphrodite sired by a M_b male, we confirmed that this cross also entails a departure from Mendelian
409 segregation, this time in favor of hermaphrodites, albeit of a lesser magnitude. Although the generality of
410 this observation still remains to be determined by careful examination of the other possible crosses (H_a
411 hermaphrodites x M_a and M_c males), it is clear that segregation distortion is a general feature of this
412 system, as was already observed in other sex determination systems causing departures from equal sex
413 ratios (e.g. KOZIELSKA *et al.* 2010). Beyond the identification of the mechanisms by which the distortions
414 arise, pinpointing the evolutionary conditions leading to their emergence will be key to understanding the
415 role they may have played in the evolution of this reproductive system.

416 More broadly, while sex and mating types are confounded in many species across the tree of life
417 and cannot be distinguished, the question of when and how sex and mating types evolve separately raises
418 several questions. The evolution of anisogamy (and hence, sexual differentiation) has been linked to that
419 of mating types (CHARLESWORTH 1978). In volvocine algae for instance, the mating-type locus in isogamous
420 species is orthologous to the pair of U/V sex chromosomes in anisogamous/oogamous species, suggesting
421 that the sex-determination system derives from the mating-type determination system (GENG *et al.* 2014).
422 From this perspective the Oleaceae family is an interesting model system, where a SI system is ancestral,
423 and in which some species have evolved sexual specialization that is aligned with the two SI phenotypes

424 (e.g. in the polygamous *F. excelsior* males belong to the H_a SI group and can only mate with hermaphrodites
425 or females of the H_b group, and the sexual system of *F. excelsior* can be viewed as subdioecy (SAUMITOU-
426 LAPRADE *et al.* 2018). In other species, sexual phenotypes are disjoint from SI specificities and led to the
427 differentiation of males and hermaphrodites. For instance, in the androdiecious *P. angustifolia* and
428 probably *F. ornus*, the male determinant is genetically independent from the SI locus but fully linked to a
429 genetic determinant causing the epistatic effect over SI (BILLIARD *et al.* 2015; VERNET *et al.* 2016). Yet other
430 species have remained perfect hermaphrodites and have no trace of sexual differentiation whatsoever (*O.*
431 *europeae*). Understanding why some species have followed one evolutionary trajectory while others have
432 followed another will be an exciting avenue for future research (BILLIARD *et al.* 2011).
433

434 ## Author Contributions

435 All authors contributed to the study presented in this paper. PS-L and PV developed, designed and oversaw
436 the study; they coordinated the cross and carried out the phenotyping and stigma tests. CG performed the
437 seedling paternity analysis. SS performed DNA extraction, library preparation and organized sequencing.
438 AC and SG constructed the data analysis pipeline and AC, SS, PS-L and VC interpreted the results and wrote
439 the manuscript.
440

441 ## Acknowledgements

442 We thank Sylvain Bertrand and Fantin Carpentier for technical help for the phenotyping and Jos Käfer for
443 scientific discussion and help in applying Sex-DETector to our material. We thank Jacques Lepart†,
444 Mathilde Dufay, Pierre Olivier Cheptou, Xavier Vekemans, Sylvain Billiard and Bénédicte Felter for scientific
445 discussions. Field and laboratory work for phenotyping were done at the Platform Terrains d'Expériences
446 (Labex CeMEB ANR-10-LABX-0004-CeMEB) of the Centre d'Ecologie Fonctionnelle et Evolutive (CEFE,
447 CNRS) with the help of Thierry Mathieu and David Degueldre and at the platform Serres cultures et terrains

expérimentaux of the Lille University with the help of Nathalie Faure and Angélique Bourceaux. We are grateful to Marie-Pierre Dubois for providing access to the microscopy facilities at the SMGE (Service des Marqueurs Génétiques en Ecologie) platform (CEFE). This work was funded by the French National Research Agency through the project 'TRANS' (ANR-11-BSV7- 013-03) and by a grant from the European Research Council (NOVEL project, grant #648321). A.C was supported by a doctoral grant from the French ministry of research. The authors also thank the Région Hauts-de-France, and the Ministère de l'Enseignement Supérieur et de la Recherche (CPER Climibio), and the European Fund for Regional Economic Development for their financial support. We also thank the HPC Computing Mésocentre of the University of Lille which provided us with the computing grid. We thank Tatiana Giraud and two anonymous referees for constructive reviews of an earlier version.

References

Badouin, H., M. E. Hood, J. Gouzy, G. Aguileta, S. Siguenza *et al.*, 2015 Chaos of Rearrangements in the Mating-Type Chromosomes of the Anther-Smut Fungus Microbotryum lychnidis-dioicae. Genetics 200**:** 1275-1284.

Barrett, S. C., 2002 The evolution of plant sexual diversity. Nature Reviews Genetics 3**:** 274-284.

Barrett, S. C. H., 1990 The evolution and adaptive significance of heterostyly. Trends in Ecology & Evolution 5**:** 144-148.

Barrett, S. C. H., 1992 Heterostylous Genetic Polymorphisms: Model Systems for Evolutionary Analysis, pp. 1-29 in *Evolution and Function of Heterostyly*, edited by S. C. H. Barrett. Springer Berlin Heidelberg, Berlin, Heidelberg.

Barrett, S. C. H., 1998 The evolution of mating strategies in flowering plants. Trends in Plant Science 3**:** 335-341.

Barrett, S. C. H., 2019 'A most complex marriage arrangement': recent advances on heterostyly and unresolved questions. New Phytologist 224**:** 1051-1067.

Besnard, G., R. Rubio de Casas, P.-A. Christin and P. Vargas, 2009 Phylogenetics of Olea (Oleaceae) based on plastid and nuclear ribosomal DNA sequences: Tertiary climatic shifts and lineage differentiation times. Annals of Botany 104**:** 143-160.

Billiard, S., L. Husse, P. Lepercq, C. Gode, A. Bourceaux *et al.*, 2015 Selfish male-determining element favors the transition from hermaphroditism to androdioecy. Evolution 69**:** 683-693.

Billiard, S., M. López-Villavicencio, B. Devier, M. E. Hood, C. Fairhead *et al.*, 2011 Having sex, yes, but with whom? Inferences from fungi on the evolution of anisogamy and mating types. Biological Reviews 86**:** 421-442.

Castric, V., and X. Vekemans, 2004 Plant self-incompatibility in natural populations: a critical assesment of recent theoretical and empirical advances. Molecular Ecology 13**:** 2873-2889.

Catchen, J. M., A. Amores, P. Hohenlohe, W. Cresko and J. H. Postlethwait, 2011 Stacks: building and genotyping Loci de novo from short-read sequences. G3 (Bethesda, Md.) 1**:** 171-182.

Chantha, S.-C., A. C. Herman, V. Castric, X. Vekemans, W. Marande *et al.*, 2017 The unusual S locus of Leavenworthia is composed of two sets of paralogous loci. New Phytologist 216**:** 1247-1255.

Chantha, S.-C., A. C. Herman, A. E. Platts, X. Vekemans and D. J. Schoen, 2013 Secondary Evolution of a Self-Incompatibility Locus in the Brassicaceae Genus Leavenworthia. PLOS Biology 11**:** e1001560.

Charlesworth, B., 1978 The population genetics of anisogamy. Journal of Theoretical Biology 73**:** 347-357.

Charlesworth, D., and B. Charlesworth, 1979 A Model for the Evolution of Distyly. The American Naturalist 114**:** 467-498.

De-Kayne, R., and P. G. D. Feulner, 2018 A European Whitefish Linkage Map and Its Implications for Understanding Genome-Wide Synteny Between Salmonids Following Whole Genome Duplication. G3 (Bethesda) 8**:** 3745-3755.

De Cauwer, I., P. Vernet, S. Billiard, C. Godé, A. Bourceaux *et al.*, 2020 Widespread coexistence of self-compatible and self-incompatible phenotypes in a diallelic self-incompatibility system in *Ligustrum vulgare* (Oleaceae). bioRxiv**:** 2020.2003.2026.009399.

De Nettancourt, D., 1977 *Incompatibility in Angiosperms*. Springer-Verlag, Berlin, Heidelberg et New York.

Diggle, P. K., V. S. Di Stilio, A. R. Gschwend, E. M. Golenberg, R. C. Moore *et al.*, 2011 Multiple developmental processes underlie sex differentiation in angiosperms. Trends in Genetics 27**:** 368-376.

Dommée, B., J. D. Thompson and F. Cristini, 1992 Distylie chez Jasminum fruticans L.: hypothèse de la pollinisation optimale basée sur les variations de l'écologie intraflorale. Bulletin de la Société Botanique de France. Lettres Botaniques 139**:** 223-234.

Dulberger, R., 1992 Floral Polymorphisms and Their Functional Significance in the Heterostylous Syndrome, pp. 41-84 in *Evolution and Function of Heterostyly*, edited by S. C. H. Barrett. Springer Berlin Heidelberg, Berlin, Heidelberg.

Dupin, J., P. Raimondeau, C. Hong-Wa, S. Manzi, M. Gaudeul *et al.*, 2020 Resolving the Phylogeny of the Olive Family (Oleaceae): Confronting Information from Organellar and Nuclear Genomes. Genes 11**:** 1508.

Geng, S., P. De Hoff and J. G. Umen, 2014 Evolution of sexes from an ancestral mating-type specification pathway. PLoS biology 12**:** e1001904-e1001904.

Goubet, P. M., H. Bergès, A. Bellec, E. Prat, N. Helmstetter *et al.*, 2012 Contrasted Patterns of Molecular Evolution in Dominant and Recessive Self-Incompatibility Haplotypes in Arabidopsis. PLOS Genetics 8**:** e1002495.

Guo, Y.-L., X. Zhao, C. Lanz and D. Weigel, 2011 Evolution of the S-locus region in Arabidopsis relatives. Plant physiology 157**:** 937-946.

Husse, L., S. Billiard, J. Lepart, P. Vernet and P. Saumitou-Laprade, 2013 A one-locus model of androdioecy with two homomorphic self-incompatibility groups: expected vs. observed male frequencies. Journal of evolutionary biology 26**:** 1269-1280.

Iwano, M., K. Ito, H. Shimosato-Asano, K.-S. Lai and S. Takayama, 2014 Self-Incompatibility in the Brassicaceae, pp. 245-254 in *Sexual Reproduction in Animals and Plants*, edited by H. Sawada, N. Inoue and M. Iwano. Springer Japan, Tokyo.

Iwano, M., and S. Takayama, 2012 Self/non-self discriminition in angiosperm self-incompatibility. Current Opinion in Plant Biology 15**:** 78-83.

Jiménez-Ruiz, J., J. A. Ramírez-Tejero, N. Fernández-Pozo, M. d. l. O. Leyva-Pérez, H. Yan *et al.*, 2020 Transposon activation is a major driver in the genome evolution of cultivated olive trees (Olea europaea L.). The Plant Genome 13**:** e20010.

Keller, B., J. D. Thomson and E. Conti, 2014 Heterostyly promotes disassortative pollination and reduces sexual interference in Darwin's primroses: evidence from experimental studies. Functional Ecology 28**:** 1413-1425.

Kozielska, M., F. J. Weissing, L. W. Beukeboom and I. Pen, 2010 Segregation distortion and the evolution of sex-determining mechanisms. Heredity 104**:** 100-112.

Krzywinski, M. I., J. E. Schein, I. Birol, J. Connors, R. Gascoyne *et al.*, 2009 Circos: An information aesthetic for comparative genomics. Genome Research.

Kubo, K.-i., T. Paape, M. Hatakeyama, T. Entani, A. Takara *et al.*, 2015 Gene duplication and genetic exchange drive the evolution of S-RNase-based self-incompatibility in *Petunia*. Nature Plants 1**:** 1-9.

Langmead, B., and S. L. Salzberg, 2012 Fast gapped-read alignment with Bowtie 2. Nature methods 9**:** 357-359.

Li, H., and R. Durbin, 2009 Fast and accurate short read alignment with Burrows-Wheeler transform. Bioinformatics 25**:** 1754-1760.

Li, J., J. M. Cocker, J. Wright, M. A. Webster, M. McMullan *et al.*, 2016 Genetic architecture and evolution of the S locus supergene in Primula vulgaris. Nature plants 2**:** 16188.

Lundqvist, A., 1956 Self-incompatibility in rye. Hereditas 42**:** 293-348.

Mariotti, R., S. Pandolfi, I. De Cauwer, P. Saumitou-Laprade, P. Vernet *et al.*, 2020 Diallelic self-incompatibility is the main determinant of fertilization patterns in olive orchards. Evolutionary Applications n/a.

Muyle, A., J. Kafer, N. Zemp, S. Mousset, F. Picard *et al.*, 2016 SEX-DETector: A Probabilistic Approach to Study Sex Chromosomes in Non-Model Organisms. Genome Biol Evol 8**:** 2530-2543.

Olofsson, J. K., I. Cantera, C. Van de Paer, C. Hong-Wa, L. Zedane *et al.*, 2019 Phylogenomics using low-depth whole genome sequencing: A case study with the olive tribe. Molecular Ecology Resources 19**:** 877-892.

Pannell, J. R., and G. Korbecka, 2010 Mating-System Evolution: Rise of the Irresistible Males. Current Biology 20**:** R482-R484.

Pannell, J. R., and M. Voillemot, 2015 Plant mating systems: female sterility in the driver's seat. Current Biology 25**:** R511-514.

Peterson, B. K., J. N. Weber, E. H. Kay, H. S. Fisher and H. E. Hoekstra, 2012 Double digest RADseq: an inexpensive method for de novo SNP discovery and genotyping in model and non-model species. PLoS One 7**:** e37135.

Rastas, P., 2017 Lep-MAP3: robust linkage mapping even for low-coverage whole genome sequencing data. Bioinformatics 33**:** 3726-3732.

Rochette, N. C., and J. M. Catchen, 2017 Deriving genotypes from RAD-seq short-read data using Stacks. Nature Protocols 12**:** 2640-2659.

Sakai, A. K., and S. G. Weller, 1999 Gender and Sexual Dimorphism in Flowering Plants: A review of Terminology, Biogeographic Patterns, Ecological Correlates, and Phylogenetic Approaches, pp. 1-31 in *Gender and Sexual Dimorphism in Flowering Plants*, edited by M. A. Geber, T. E. Dawson and L. F. Delph. Springer Berlin Heidelberg, Berlin, Heidelberg.

Saumitou-Laprade, P., P. Vernet, A. Dowkiw, S. Bertrand, S. Billiard *et al.*, 2018 Polygamy or subdioecy? The impact of diallelic self-incompatibility on the sexual system in Fraxinus excelsior (Oleaceae). Proceedings. Biological sciences 285**:** 20180004.

Saumitou-Laprade, P., P. Vernet, C. Vassiliadis, Y. Hoareau, G. de Magny *et al.*, 2010 A self-incompatibility system explains high male frequencies in an androdioecious plant. Science 327**:** 1648-1650.

Saumitou-Laprade, P., P. Vernet, X. Vekemans, S. Billiard, S. Gallina *et al.*, 2017 Elucidation of the genetic architecture of self-incompatibility in olive: Evolutionary consequences and perspectives for orchard management. Evolutionary Applications**:** 1-14.

Tsagkogeorga, G., V. Cahais and N. Galtier, 2012 The population genomics of a fast evolver: high levels of diversity, functional constraint, and molecular adaptation in the tunicate Ciona intestinalis. Genome Biol Evol 4**:** 740-749.

Unver, T., Z. Wu, L. Sterck, M. Turktas, R. Lohaus *et al.*, 2017 Genome of wild olive and the evolution of oil biosynthesis. Proceedings of the National Academy of Sciences of the United States of America 114**:** E9413-e9422.

Vassiliadis, C., P. Saumitou-Laprade, J. Lepart and F. Viard, 2002 High male reproductive success of hermaphrodites in the androdioecious Phillyrea angustifolia. Evolution 56**:** 1362-1373.

Vernet, P., P. Lepercq, S. Billiard, A. Bourceaux, J. Lepart *et al.*, 2016 Evidence for the long-term maintenance of a rare self-incompatibility system in Oleaceae. New Phytologist 210**:** 1408-1417.

Wallander, E., and V. A. Albert, 2000 Phylogeny and classification of Oleaceae based on rps16 and trnL-F sequence data. American Journal of Botany 87**:** 1827-1841.

Wright, S., 1939 The Distribution of Self-Sterility Alleles in Populations. Genetics 24**:** 538-552.

Table 1. Comparison of the sex-averaged, male and female linkage maps. The values in this table are computed without the outliers SNPs markers at the extremity of the linkage groups.

			Sex-averaged map			Paternal map			Maternal map		
Linkage group	**Number of SNPs**	**Number of SNPs (without outliers)**	**LG length (cM)**	**SNPs/cM**	**average intermarker distance**	**LG Length (cM)**	**SNPs/cM**	**average intermarker distance**	**LG Length (cM)**	**SNPs/cM**	**average intermarker distance**
1	854	839	75.78	11.07	0.09	79.30	10.58	0.09	92.11	9.11	0.11
2	633	621	23.90	25.98	0.10	35.00	17.74	0.12	22.73	27.32	0.11
3	676	676	74.50	9.07	0.11	61.94	10.91	0.09	85.42	7.91	0.13
4	535	535	68.07	7.86	0.13	71.63	7.47	0.13	69.82	7.66	0.13
5	502	494	56.02	8.82	0.11	50.58	9.77	0.10	67.84	7.28	0.14
6	877	877	96.89	9.05	0.11	90.81	9.66	0.10	103.63	8.46	0.12
7	609	601	64.14	9.37	0.11	68.93	8.72	0.11	64.99	9.25	0.11
8	486	479	62.71	7.64	0.13	91.89	5.21	0.19	119.25	4.02	0.25
9	408	406	63.28	6.42	0.16	56.06	7.24	0.14	71.04	5.72	0.18
10	1365	1361	110.69	12.30	0.08	121.95	11.16	0.09	112.38	12.11	0.08
11	793	783	91.66	8.54	0.12	80.40	9.74	0.10	108.84	7.19	0.14
12	973	969	77.12	12.56	0.08	91.52	10.59	0.09	88.09	11.00	0.09
13	849	848	77.40	10.96	0.09	77.29	10.97	0.09	80.77	10.50	0.10
14	566	565	62.12	9.10	0.11	72.25	7.82	0.13	71.39	7.91	0.13
15	750	747	76.92	9.71	0.10	82.98	9.00	0.11	96.01	7.78	0.13
16	591	589	53.53	11.00	0.09	56.93	10.35	0.10	69.56	8.47	0.12
17	613	613	76.52	8.01	0.13	70.58	8.69	0.12	83.94	7.30	0.14
18	660	659	76.22	8.65	0.12	77.26	8.53	0.12	81.99	8.04	0.12
19	806	806	69.29	11.63	0.09	91.10	8.85	0.11	79.49	10.14	0.10
20	547	531	56.26	9.44	0.11	67.56	7.86	0.13	62.91	8.44	0.12
21	479	476	54.86	8.68	0.12	69.49	6.85	0.15	54.14	8.79	0.11
22	550	544	57.05	9.54	0.11	55.64	9.78	0.10	61.44	8.85	0.11
23	690	684	61.64	11.10	0.09	67.10	10.19	0.10	66.42	10.30	0.10
average	687	682	68.98	10.28	0.11	73.40	9.46	0.11	78.88	9.29	0.12

608 **Figure 1.** *Phillyrea angustifolia* sex-averaged linkage map showing the grouping and position of 15703
609 SNPs. The length of each of the 23 linkage groups is indicated by the vertical scale in cM. The markers
610 strictly linked to sex and self-incompatibility (SI) phenotypes are shown in red. Markers that were clearly
611 outliers at the end of some linkage groups were removed (see Table1, Figure S1).

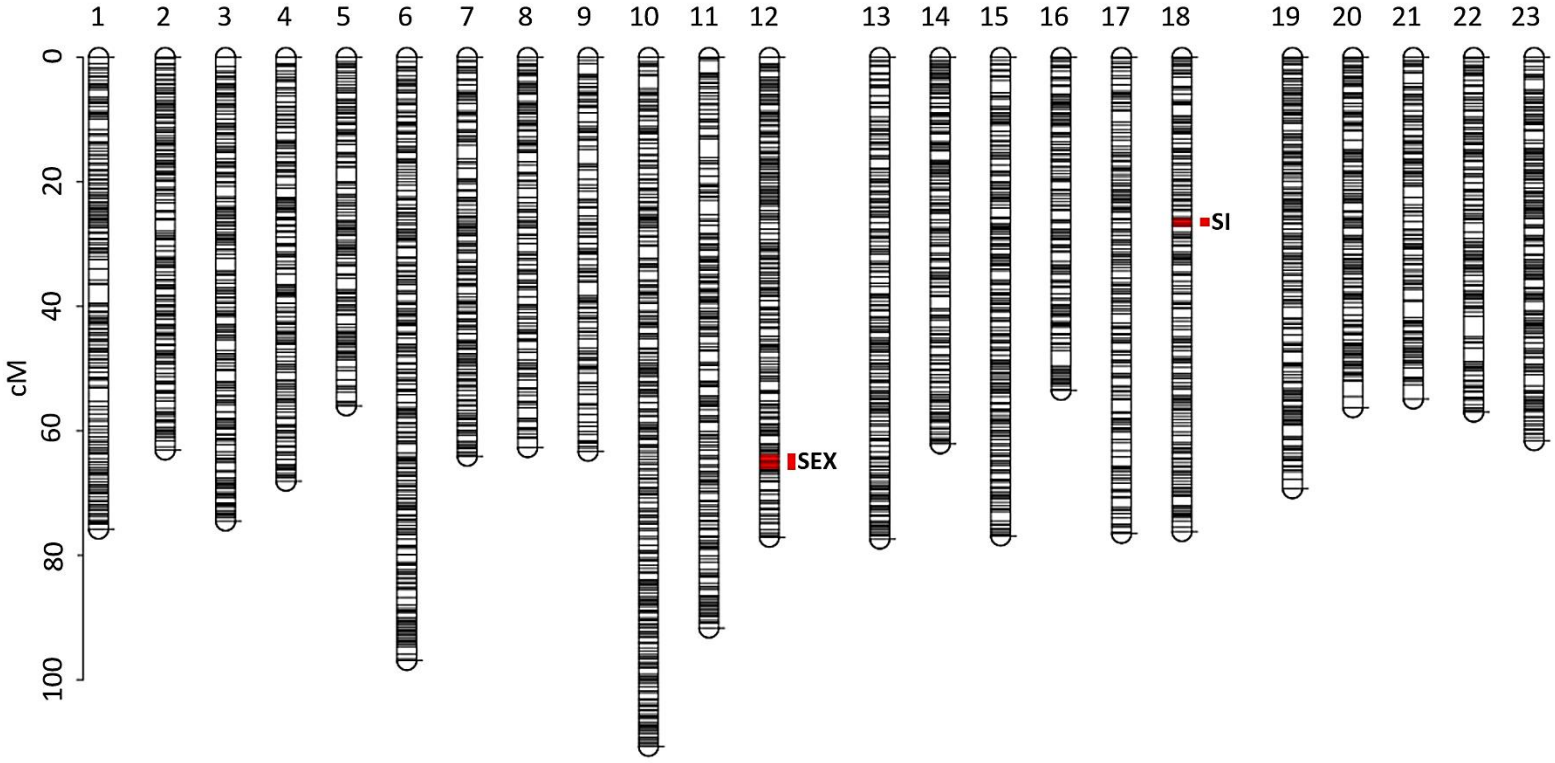

Figure 2. Synteny plot identifying homologous *P. angustifolia* linkage groups (LG, scale in cM) with olive tree chromosomes (Chr, scale in Mb). Lines connect markers in the *P. angustifolia* linkage map with their best BLAST hit in the *O. europea* genome and are colored according to the linkage group. Variation of the density of loci in bins of 3.125cM along linkage groups and 1 Mbp along chromosomes is shown in the inner circle as a black histogram.

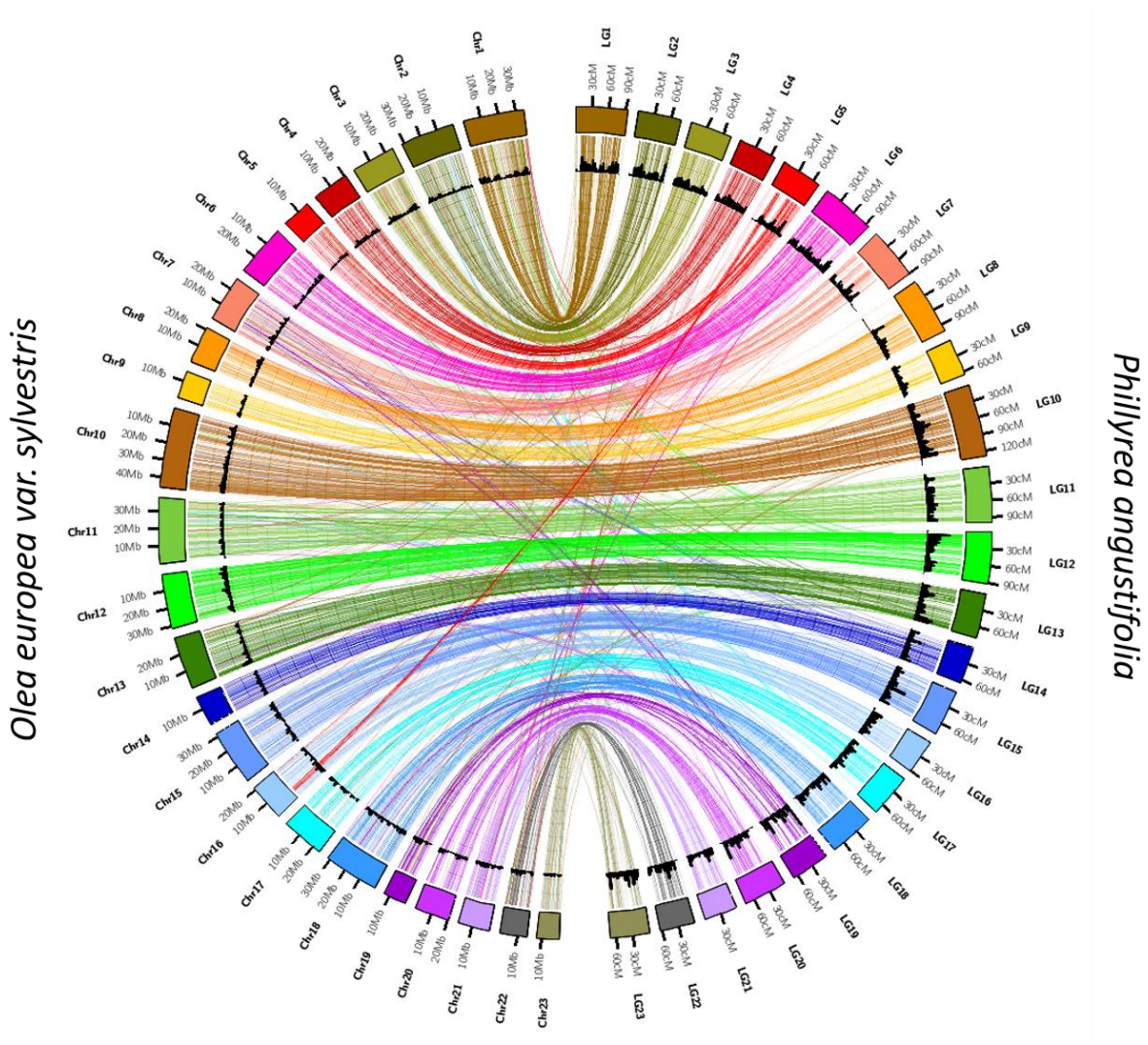

618 **Figure 3.** Visualization of chromosome-scale synteny by comparing the location of markers along the *P.*
619 *angustifolia* linkage groups (LG, scale in cM) with the location of their best BLAST hit along the homologous
620 olive tree chromosome (Chr, scale in Mbp). The vertical lines on LG12 and LG18 indicate the position of
621 markers strictly associated with sex and SI phenotypes in *P. angustifolia*, respectively. The horizontal line
622 on Chr18 indicates the chromosomal region containing the SI locus in *Olea europaea* according to Mariotti
623 *et al.* (2020).

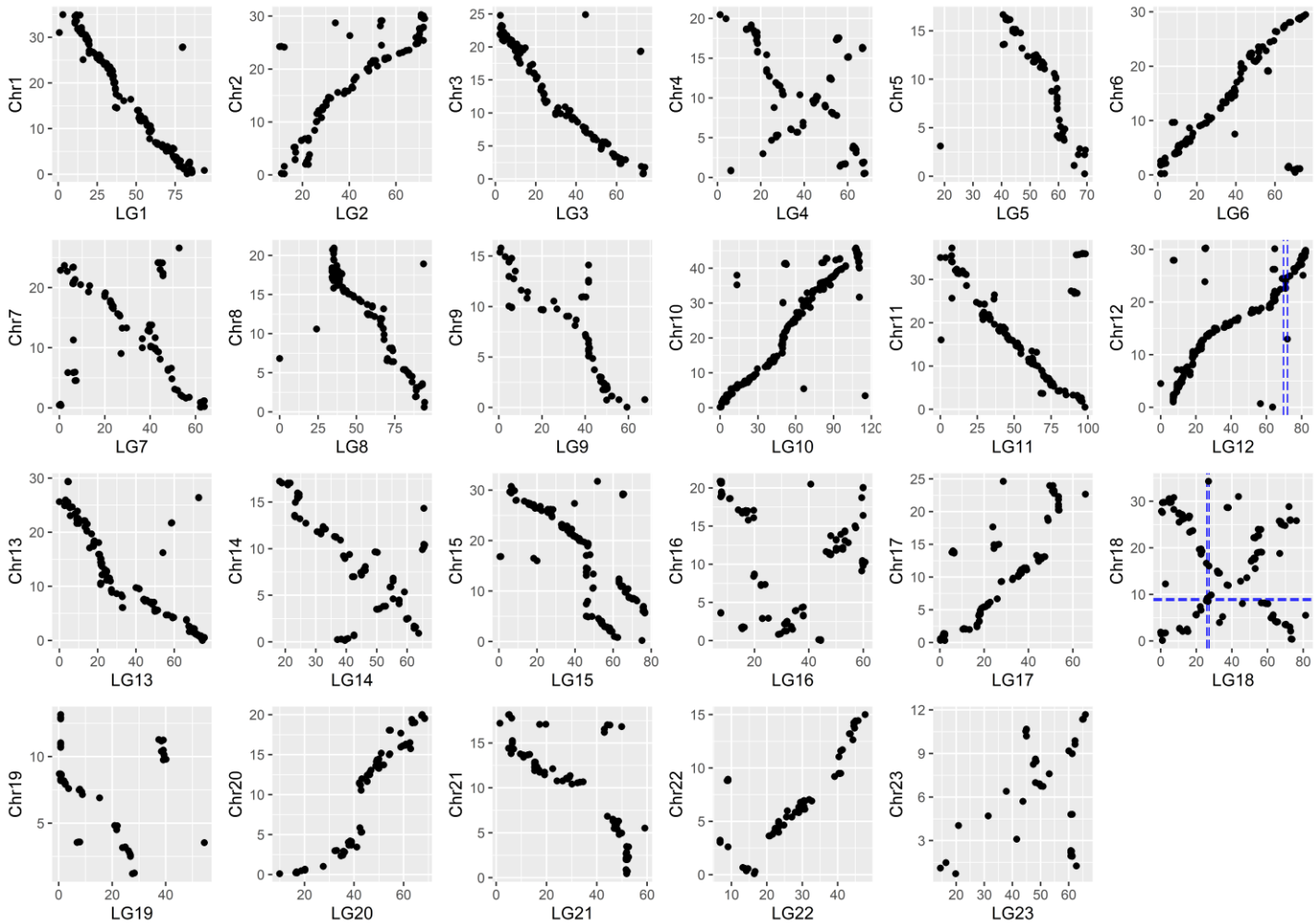

624

Figure 4. Synteny plot between the *P. angustifolia* linkage group 12 (scale in cM) and the olive tree chromosomes 12 and a series of unanchored scaffolds (scale in Mb). Lines connect markers in the *P. angustifolia* linkage map with their best BLAST hit in the *O. europea* genome. Green lines correspond to markers with autosomal inheritance. Black lines correspond to markers which strictly cosegregate with sex phenotypes (males *vs.* hermaphrodites). Red lines correspond to markers with strong but partial (95%) association with sex. Variation of the density of loci in bins of 3.125cM along linkage groups and 1 Mbp along chromosomes is shown in the inner circle as a black histogram.

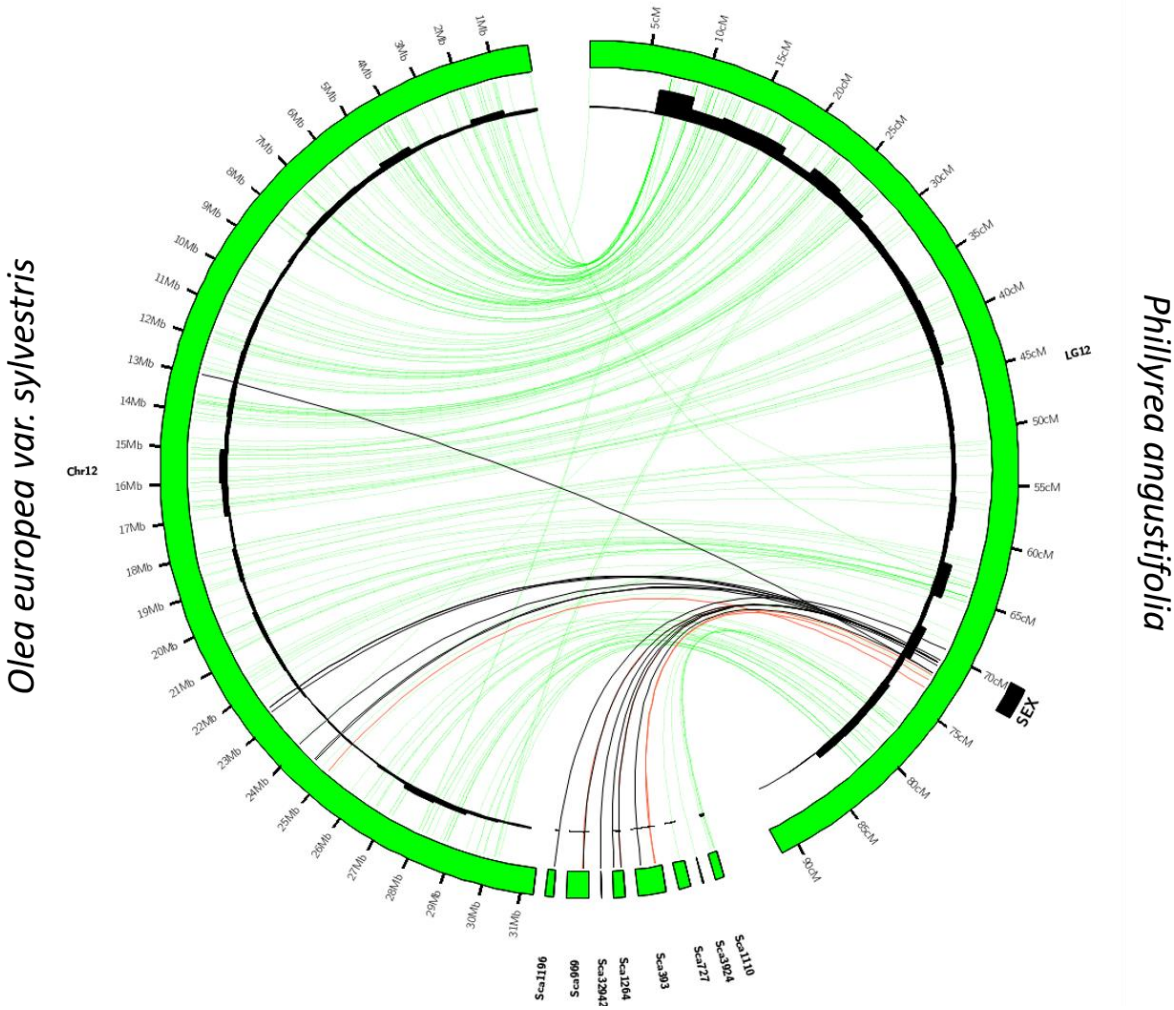
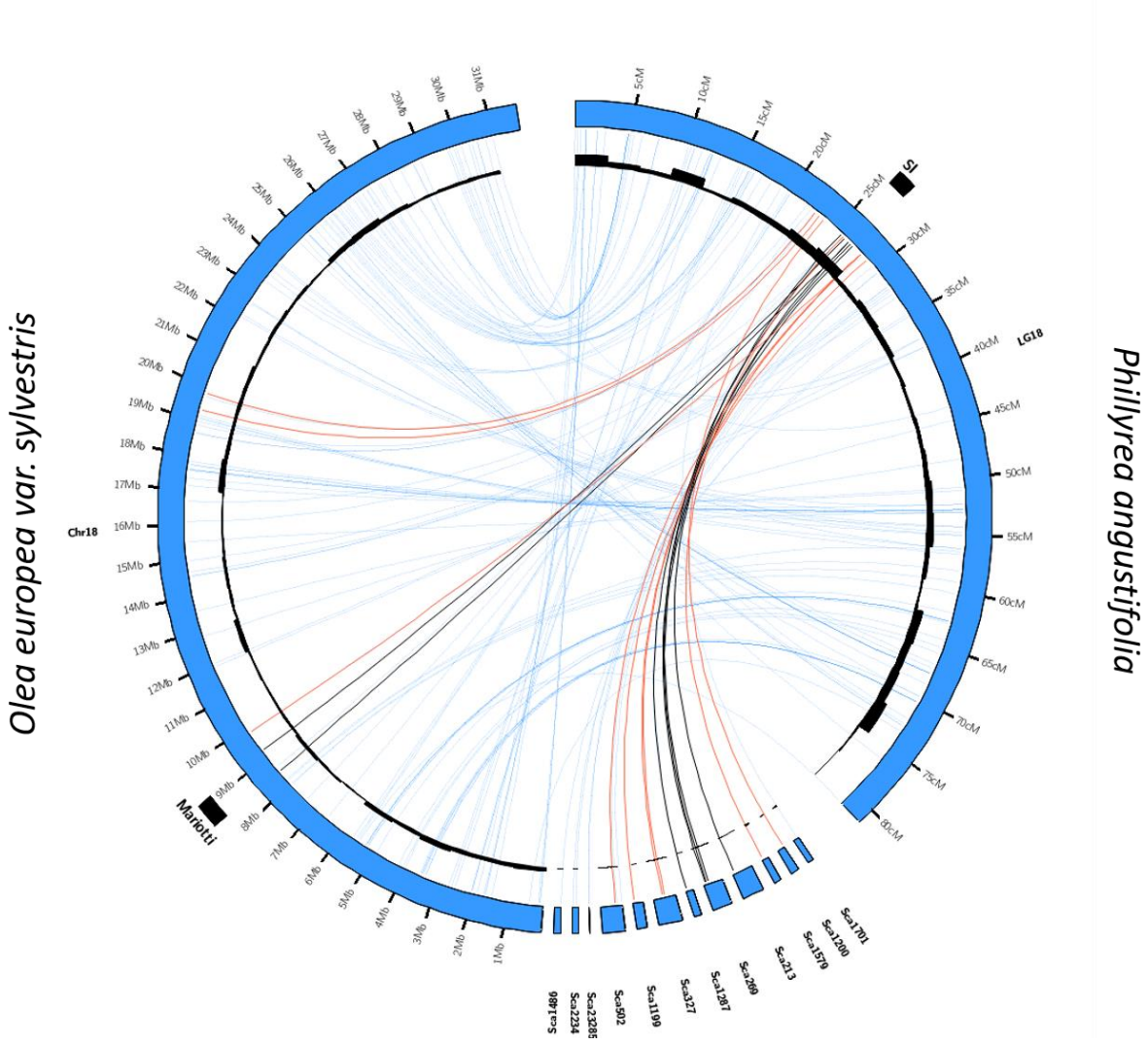
Figure 5. Synteny plot between the *P. angustifolia* linkage group 18 (scale in cM) and the olive tree chromosomes 18 and a series of unanchored scaffolds (scale in Mb). Lines connect markers in the *P. angustifolia* linkage map with their best BLAST hit in the *O. europea* genome. Blue lines correspond to markers with autosomal inheritance. Black lines correspond to markers which strictly cosegregate with SI phenotypes (H_a *vs.* Hb). Red lines correspond to markers with strong but partial (95%) association with SI. The region found to be genetically associated with SI in the olive tree by Mariotti *et al.* (2020) is shown by a black rectangle. Variation of the density of loci in bins of 3.125cM along linkage groups and 1 Mbp along chromosomes is shown in the inner circle as a black histogram.